

# Nitsche Method for non-Fourier Heat Conduction

Martin Sýkora

October 2024

## 1 Introduction

Heat conduction is often described by the Fourier law

$$\mathbf{q} = -k\nabla T,$$

which states that the heat flux  $\mathbf{q}$  is proportional to the gradient of temperature  $T$ . The ratio is given by heat conductivity  $k$ . While this description is sufficient in many conditions, there are some settings, where a more detailed approach is needed, for instance heat conduction at very small size scale. A class of such approaches is called phonon hydrodynamics, see for instance [1, 2]. A new addition to the phonon hydrodynamics equations has been developed in [3]. This approach, derived from phonon kinetic theory through a first-order asymptotic expansion in the irreversible part and the Poisson projection in the reversible part, is rather complex. It incorporates both convection and diffusion, and therefore it highly resembles compressible Navier-Stokes equations. The equations read

$$\partial_t e = -\partial_i(c^2 m_i), \tag{1}$$

$$\begin{aligned} \partial_t m_i = & -\partial_i p - \partial_j \left( \frac{3c^2}{4e} m_i m_j \right) \\ & - \frac{1}{\tau_R} m_i + \frac{\tau c^2}{5} \partial_j \left( \partial_j m_i + \partial_i m_j - \frac{2}{3} \nabla \cdot \mathbf{m} \delta_{ij} \right) \end{aligned} \tag{2}$$

with pressure

$$p \approx \frac{e}{3} - \frac{c^2 \mathbf{m}^2}{4e}. \tag{3}$$

Here,  $\tau^{-1}, \tau_R$  are relaxation times,  $c$  is the sound speed and the unknowns  $e, \mathbf{m}$  stand for energy and phonon momentum. In [3], the authors performed numerical computations to demonstrate the effects the model can describe, like temperature drop past a cylindrical obstacle or von Kármán vortex street. The computations were non-physical (material parameters used for computations were nonrealistic) and should be understood as theoretical experiments. However, even non-physical computations should not neglect the effects of boundary

conditions (BCs). If one is interested in the behaviour of certain equations, they need to check, whether the result is dependent on the BCs used.<sup>1</sup> Therefore, the authors used both no-slip BCs, which are easy and straightforward to apply and slip BCs, applied by the so-called Nitsche method.<sup>2</sup> This method, however, contains a parameter  $\beta$ , which was for simplicity ignored (i.e. set to zero) by the authors. In this text we show the effects of non-zero  $\beta$ .

## 2 Results

### 2.1 Nitsche method

As the equations are similar to Navier-Stokes equations, the inspiration for the Nitsche method could be taken from [5, 6]. In [3] and [7], this is done by adding

$$\int \frac{\Theta}{\gamma(1-\Theta)} \mathbf{m}_\tau \cdot \mathbf{v}_\tau dS - \int (\mathbf{T}(e, \mathbf{m})\mathbf{n})_n \cdot \mathbf{v}_n dS + \int \mathbf{m}_n \cdot (\tilde{\mathbf{T}}(f, \mathbf{v})\mathbf{n})_n dS. \quad (4)$$

to the weak formulation of the equations. Here,  $\mathbf{T}$  and  $\tilde{\mathbf{T}}$  stand for

$$\mathbf{T}(f, \mathbf{v}) = - \left( \frac{f}{3} - \frac{c^2 \mathbf{v}^2}{4f} \right) \mathbf{I} + \frac{c^2 \tau}{5} \left( (\nabla \mathbf{v} + \nabla \mathbf{v}^\top) - \frac{2}{3} \text{div}(\mathbf{v}) \mathbf{I} \right) \quad (5)$$

and

$$\tilde{\mathbf{T}}(f, \mathbf{v}) = - \left( \frac{f}{3} - \frac{c^2 \mathbf{v} \cdot \mathbf{m}_0}{4e_0} \right) \mathbf{I} + \frac{c^2 \tau}{5} \left( (\nabla \mathbf{v} + \nabla \mathbf{v}^\top) - \frac{2}{3} \text{div}(\mathbf{v}) \mathbf{I} \right), \quad (6)$$

respectively.<sup>34</sup> Here  $e, \mathbf{m}$  are the unknown functions and  $f, \mathbf{v}$  the test functions. In this text we add

$$\frac{\beta \tau c^2}{5h} \int \mathbf{m} \cdot \mathbf{v} dS, \quad (7)$$

where  $h$  is the maximum edge length.

### 2.2 Setting and results

The overall setting is described in figure 1. In order to compare results, we plot the momentum over a vertical line just right of the cylindrical obstacle.

Let us compute the momentum flow through the cylinder boundary (should equal zero) for different  $\beta$  over the same mesh, compared to the inlet flow. This result is summarised in figure 2. One can see that with increasing  $\beta$ , the flux through wall decreases. Higher  $\beta$  can lead to higher computational requirements, however, in this simple setting the differences are negligible. In the following paragraphs, we compare choice  $\beta = 0$  from [3] and  $\beta = 1000$ .

<sup>1</sup>For example the famous Poiseuille flow (parabolic velocity profile in a pressure-drop-driven flow in a straight channel) is *enforced* by no-slip BCs. For different BCs, the result, i.e. the velocity profile, could be completely different.

<sup>2</sup>Note, however, that there exist other approaches to BCs for phonon hydrodynamics; for instance the BCs presented in [4].

<sup>3</sup>Note that a linearisation in pressure was used.

<sup>4</sup>We are using non-symmetric Nitsche method.

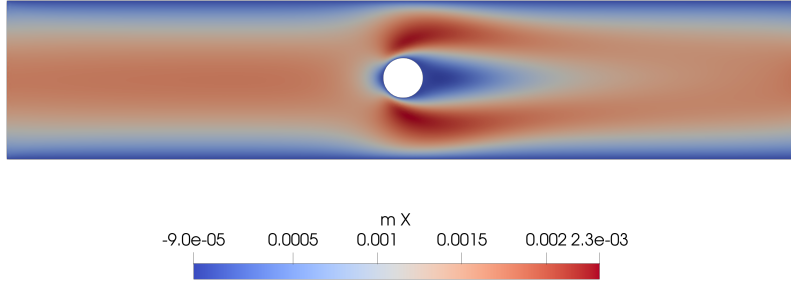


Figure 1: The x-direction phonon momentum in a flow past a cylinder.

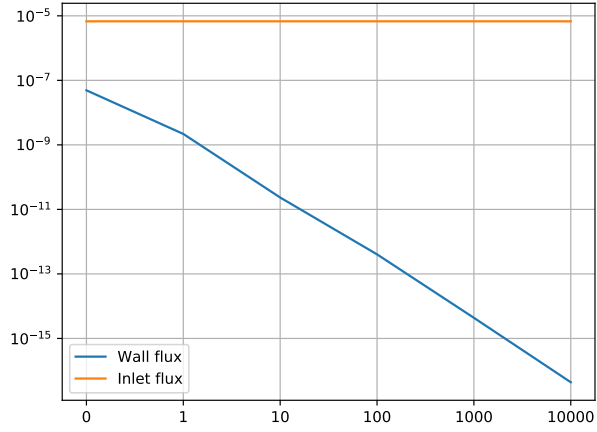


Figure 2: Flux through the cylinder wall (blue line) and inlet boundary (orange line). With increasing  $\beta$ , the flux through wall diminishes.

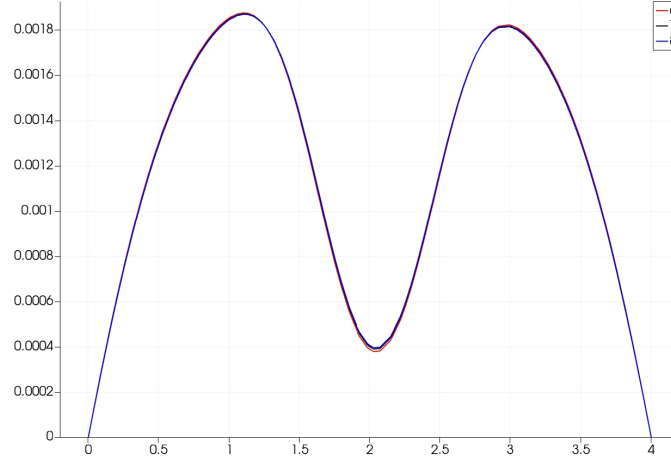


Figure 3: Phonon momentum past a cylindrical obstacle with  $\beta = 0$  for various levels of mesh refinement, red = level six, black = level seven, blue = level eight. Higher level means finer mesh.

### 2.2.1 Case $\beta = 0$

As the BC is not exact (see the large flux through cylinder wall), we need to refine it a lot, at least around the cylinder, until the solutions converge. We perform refinements, each level of refinement shortening the edge length roughly two times. Figure 3 shows the convergence of level six, seven and eight refinement. We can see a small difference between levels six and seven and a (near) convergence between levels seven and eight. Therefore one needs to decrease the edge length roughly  $2^7$  times to reach convergence.

### 2.2.2 Case $\beta = 1000$

We perform the same test with two differences. First, the refinement should not be performed locally around the cylinder but globally as the stabilisation parameter depends on the maximum edge length  $h$  over the whole mesh. Second, we only compare zeroth and first refinement. The result is shown in figure 4. The solutions are nearly the same, so the convergence happens even without refinement. To conclude, higher  $\beta$  results in much faster convergence. Also note the different solution from case  $\beta = 0$  – the saddle momentum is much lower here, actually negative. We now compare the solution for  $\beta = 1000$  and  $\beta = 10^9$  to verify that the former choice is already large enough and gives the correct result. This is shown in figure 5 and indeed, the results are undistinguishable.

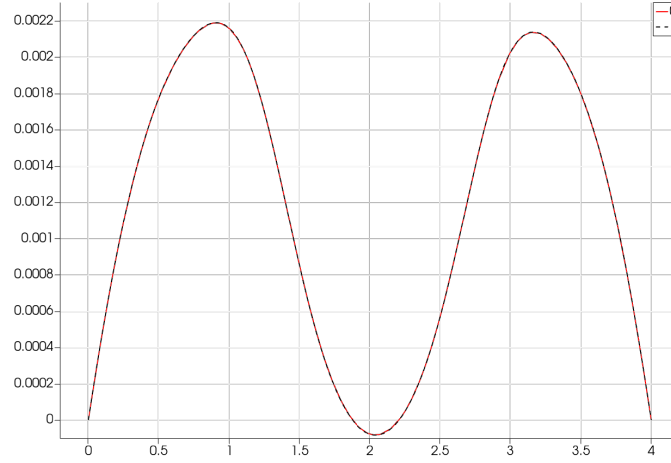


Figure 4: Phonon momentum past a cylindrical obstacle with  $\beta = 1000$  for various levels of mesh refinement, red = level zero, black dashed = level one. Higher level means finer mesh. Refinements are performed over the whole mesh as the additional stabilisation term depends on mesh size maximum over the whole mesh.

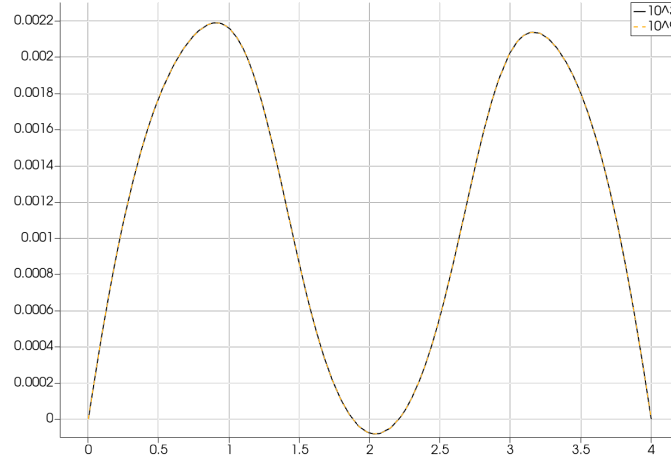


Figure 5: Phonon momentum past a cylindrical obstacle with  $\beta = 10^3$  (black) and  $\beta = 10^9$  (orange dashed). One can see a convergence in  $\beta$  as the two results are equal.

### 3 Conclusion

This text does not have the ambition to fully describe the ideal choice of BCs. A few remarks could be, however, inferred from the above results:

1. The choice of  $\beta$  does matter.
2. Higher  $\beta$  leads to lower wall flux, other quantities being the same, i.e. higher  $\beta$  give more accurate BCs.
3. The difference between the BCs for different betas can have a serious impact on the solution globally.
4. It is not necessary to take  $\beta$  extremely high. The solutions are not affected by its change for high enough values.
5. With a correct choice of *beta* (here 1000), non-symmetric Nitsche method gives reasonable low wall flux and convergence speed.

### References

- [1] R. A. Guyer and J. A. Krumhansl. Solution of the linearized phonon Boltzmann equation. *Physical review*, 148(2), 1966.
- [2] Y. Guo and M. Wang. Phonon hydrodynamics and its applications in nanoscale heat transport. *Physics Reports*, 595:1–44, 2015.
- [3] M. Sýkora, M. Pavelka, L. Restuccia, and D. Jou. Multiscale heat transport with inertia and thermal vortices. *Physica Scripta*, 98(10):105234, 2023.
- [4] Y. Guo and M. Wang. Phonon hydrodynamics for nanoscale heat transport at ordinary temperatures. *Physical Review B*, 97(035421), 2018.
- [5] R. Chabiniok, J. Hron, A. Jarolímová, J. Málek, K. R. Rajagopal, K. Rajagopal, H. Švihlová, and K. Tůma. A benchmark problem to evaluate implementational issues for three-dimensional flows of incompressible fluids subject to slip boundary conditions. *Applications in Engineering Science*, 6:100038, 2021.
- [6] R. Chabiniok, J. Hron, A. Jarolímová, J. Málek, K.R. Rajagopal, K. Rajagopal, H. Švihlová, and K. Tůma. Three-dimensional flows of incompressible navier–stokes fluids in tubes containing a sinus, with varying slip conditions at the wall. *International Journal of Engineering Science*, 180:103749, 2022.
- [7] M. Sýkora. *Non-equilibrium Thermodynamics of Hyperbolic Systems*. PhD thesis, Faculty of Mathematics and Physics, Charles University, Czechia, 2024.